XX IMEKO World Congress
Metrology for Green Growth
September 9–14, 2012, Busan, Republic of Korea

USAGE OF TWO-CENTER BASIS FUNCTION NEURAL CLASSIFIERS IN COMPACT SMART RESISTIVE SENSORS

M. Kowalewski, Z. Czaja

Faculty of Electronics, Telecommunications and Informatics, Gdansk University of Technology, Poland,
ul. G. Narutowicza 11/12, 80-233 Gdansk

Abstract: A new solution of the smart resistance sensor with the Two-Center Basis Function (TCBF) neural classifier, for which the resistance sensor is a component of an anti-aliasing filter of an ADC is proposed. The temperature measurement procedure is based on excitation of the filter by square impulses, sampling time response of the filter and processing measured voltage values by the TCBF classifier. All steps of the measurement procedure can be realized by the microcontroller and its internal devices.

Keywords: microcontrollers, smart resistive sensors, neural networks, fault identification.

1. INTRODUCTION

At present, more and more sensors are produced as smart sensors in one chip with digital interfaces. But, e.g. many temperature sensors cannot be made in this technology, what follows from the limited range of operating temperature of the chip. Hence, resistance sensors (e.g. the Pt100), or thermocouples are still used.

In typical measurement applications of resistance sensors, the resistance is measured on the basis of resistance bridges and high resolution Σ-Δ ADCs [1], or with use of circuits in which the sensor is stimulated by a DC current source and the voltage on the sensor is amplified, filtered and next measured by an ADC [2]. These applications are complex and they are not very suitable for simple measurement systems with a battery power supply, often working as endpoints in wireless sensor networks.

Obviously, there are solutions for which resistive sensors [3,4], differential resistive sensors [5] and resistive sensor bridges [6,7] are directly connected to a microcontroller without any intermediate active components. In all these cases resistance measurements are burdened with high uncertainty, which follows from parameters of the microcontroller pin and influence of disturbances, because the measurement circuit is not equipped with an anti-aliasing filter. Therefore, a new compact smart resistance sensor with the TCBF neural classifier [8] with identification purposes is proposed in the paper.

The main idea of the new method depends on placement of the resistance sensor in the structure of the anti-aliasing filter of the ADC [9] and obtaining information about temperature from expanded TCBF classifier with parameter identification capabilities.

2. THE ARCHITECTURE OF THE SENSOR

The microcontroller is the main part of the sensor. Its internal 8-bit timer controls the duration time of two square impulses, which excite the 2nd-order low-pass Sallen-Key filter with the gain equal to 3 (Fig. 1). The excitation signal is generated on the OC0 pin. It passes through the inverter built from an IRF7105PBF.

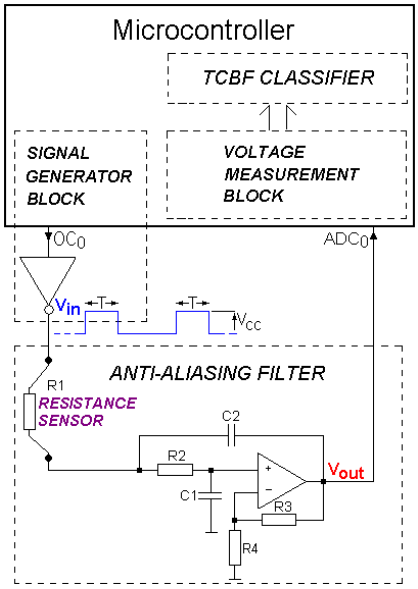

Fig. 1. A compact smart resistance sensor controlled by the microcontroller.

As an example of the resistance sensor the Pt100 sensor is used, marked as R_1. Hence, nominal values of the anti-aliasing filter are the following: R_1 (Pt100) = 110 Ω, what corresponds to about 26 °C (according to PN-EN 60751+A2), R_2 = 110 Ω, R_3 = 20 kΩ, R_4 = 10 kΩ, C_1 = 2,038 μF, C_2 = 1,022 μF. It is assumed that values of R_1 change from 0.2 to 3 of its nominal value, what corresponds to temperatures from about –192 °C to 651 °C.

The time response of the anti-aliasing filter for the first square impulse is sampled by the internal 10-bit ADC at moment t_1 (the $u(t_1)$ sample) and for the second one at moment t_2 (the $u(t_2)$ sample) established by the 16-bit timer, as in [9]. The samples $u(t_1)$ and $u(t_2)$ are treated as coordinates of the measurement point **x** and are applied to the input of the TCBF classifier in order to determine the temperature.

3. THE TCBF DESCRIPTION

The main reason of introduction of TCBF follows from the fact that usage of conventional one-center Basis Functions, either in Radial (RBF) or Ellipsoidal (EBF) form, in microcontroller based systems is difficult due to high memory demands of RBF and EBF classifiers designed for diagnostic purposes [10]. The problem is especially noticeable in detection of parametric faults. These faults are caused by variations of one or more technical object's parameters outside tolerance range and are represented in a measurement space in the form of a family of identification curves [10]. Assumption of disturbances, measurement errors and parameter tolerances causes dispersion of these curves and requires usage of neural classifiers with generalization capabilities. As an example, a family of dispersed identification curves for the anti-aliasing filter used in the smart resistance sensor is shown in Fig. 2. Voltage samples $u(t_1)$ and $u(t_2)$ are coordinates of the measurement space. Parametric faults in the range ± 50 % with reference to nominal values and parameter tolerances not greater than 2 % were assumed.

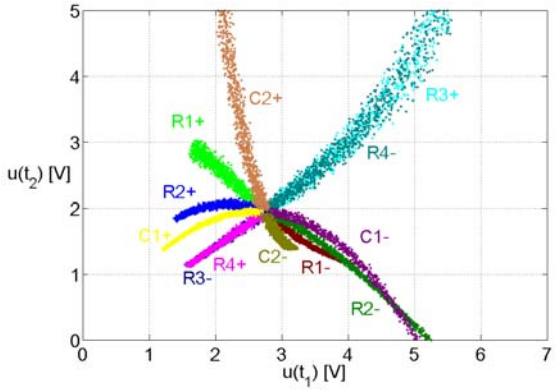

Fig. 2. Exemplary family of dispersed identification curves.

Since a shape of a dispersed identification curve has the form of a highly stretched cluster, its transformation by hidden layer neurons of RBF or EBF neural classifier requires application of many basis functions. High memory demands of these classifiers can be decreased at the cost of slightly increased computational complexity with use of TCBFs, which are used in place of RBFs or EBFs.

The TCBF maps the space around a line segment with endpoints $\mathbf{c}^{(1)}$ and $\mathbf{c}^{(2)}$ with the following equation [8]:

$$y(\mathbf{x}) = \exp\left(-\frac{1}{2s^2(\mathbf{x})} \left(\mathbf{x}-\mathbf{w}(\mathbf{x})\right)^{\mathrm{T}} \mathbf{C} \left(\mathbf{x}-\mathbf{w}(\mathbf{x})\right) \right), \quad (1)$$

where: $\mathbf{x} = [x_1, \ldots, x_n]$ is an input vector (in our case $n = 2$, $x_1 = u(t_1)$, $x_2 = u(t_2)$), $\mathbf{w}(\mathbf{x}) = [w_1(\mathrm{x}), \ldots, w_n(\mathrm{x})]$ are *center functions* depending on coordinates of centers $\mathbf{c}^{(1)}$ and $\mathbf{c}^{(2)}$, $s(\mathbf{x})$ is a *scaling function* describing the identification curve dispersion changing form σ_1 in $\mathbf{c}^{(1)}$ to σ_2 in $\mathbf{c}^{(2)}$ and $\mathbf{C} = [c_{ij}]_{n\times n}$ is a scaling matrix. Exemplary TCBF with parameters: $\mathbf{c}^{(1)} = (-2, 0)$, $\mathbf{c}^{(2)} = (2, 2)$, $\sigma_1 = 1$, $\sigma_2 = 1.25$, $c_{11} = c_{22} = 1.28$, $c_{12} = c_{21} = 0.28$ in 2-dimensional space with coordinates x_1 and x_2 is shown in Fig. 3.

The TCBF calculation algorithm presented in Fig. 4 indicates that in order to obtain value of TCBF one should evaluate additional *normalizing function* $h(\mathbf{x})$. The method depends on relation between values σ_1 and σ_2. If $\sigma_1 = \sigma_2$ then the following equation is used [8]:

$$h(\mathbf{x}) = \frac{\left(\mathbf{c}^{(2)}-\mathbf{c}^{(1)}\right)^{\mathrm{T}} \mathbf{C} \left(\mathbf{x}-\mathbf{c}^{(1)}\right)}{\left(\mathbf{c}^{(2)}-\mathbf{c}^{(1)}\right)^{\mathrm{T}} \mathbf{C} \left(\mathbf{c}^{(2)}-\mathbf{c}^{(1)}\right)}, \quad 0 \le h(\mathbf{x}) \le 1. \quad (2)$$

Otherwise, if $\sigma_1 \neq \sigma_2$, the normalizing function $h(\mathbf{x})$ is evaluated from the equation [8]

$$h(\mathbf{x}) = \frac{\left(\mathbf{x}-\mathbf{c}^{(0)}\right)^{\mathrm{T}} \mathbf{C} \left(\mathbf{x}-\mathbf{c}^{(1)}\right)}{\left(\mathbf{x}-\mathbf{c}^{(0)}\right)^{\mathrm{T}} \mathbf{C} \left(\mathbf{c}^{(2)}-\mathbf{c}^{(1)}\right)}, \quad 0 \le h(\mathbf{x}) \le 1, \quad (3)$$

where $\mathbf{c}^{(0)}$ is the apex of the elliptic cone into which two ellipsoids $f_1(\mathbf{x})$ and $f_2(\mathbf{x})$ are inscribed, as discussed in [8].

The task of the function $h(\mathbf{x})$ in the first case ($\sigma_1 = \sigma_2$) is to normalize distance between two parallel hyperplanes π_1 and π_2, which cross centres $\mathbf{c}^{(1)}$ and $\mathbf{c}^{(2)}$. However in the second case ($\sigma_1 \neq \sigma_2$) function $h(\mathbf{x})$ normalizes distance between ellipsoids $f_1(\mathbf{x})$ and $f_2(\mathbf{x})$.

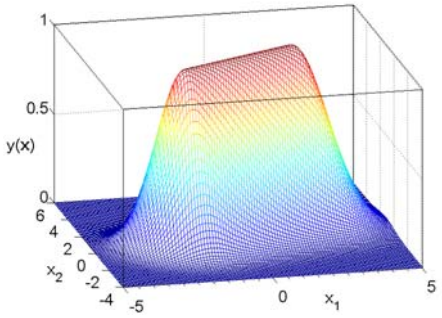

Fig. 3. The exemplary Two-Center Basis Function.

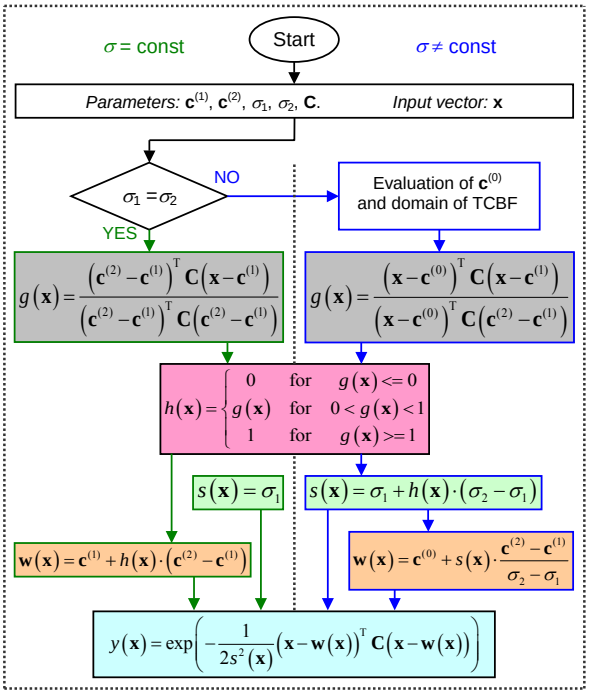

Fig. 4. The TCBF calculation algorithm.

4. THE TCBF CLASSIFIER

A set of TCBFs can be used as hidden layer neurons in a TCBF classifier destined for detection and localization of parametric faults in a technical object under test. The architecture of the classifier is presented in Fig. 5.

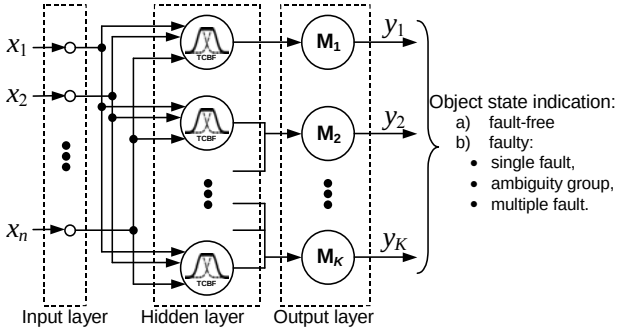

Fig. 5. The architecture of the TCBF classifier.

The classifier has two layers of neurons. TCBFs are placed in the hidden layer and are assigned to identification curves. Each neuron in the output layer marked as M_k ($0 \le k \le K$) produce maximum value of all TCBFs outputs assigned to identification curve k. Hence, an element y_k in the output vector $\mathbf{y} = [y_1, \ldots, y_K]$ gives an information about a distance in the n-dimensional space between the point $\mathbf{x}$ and the identification curve k. This information is given as a value in the range (0, 1]. If the point $\mathbf{x}$ is placed near the identification curve k then value of y_k is close to 1. The value y_k decreases to 0, if point $\mathbf{x}$ is distant from the curve.

Information about the state of the object under test can be obtained by analysing values in the output vector $\mathbf{y}$ of the classifier as was described in [11]. The TCBF classifier is able to detect if the object is fault-free or faulty and in second case distinguish single parametric fault, ambiguity group and multiple fault.

5. TEMPERATURE IDENTIFICATION

The classifier shown in Fig. 5 needs to be expanded in order to enable identification of parameters of an object. For simplicity we assume situation where only one parameter R_1 (Pt100) of an object must be identified. The architecture of the new expanded TCBF classifier with parameter identification capability is presented in Fig. 6.

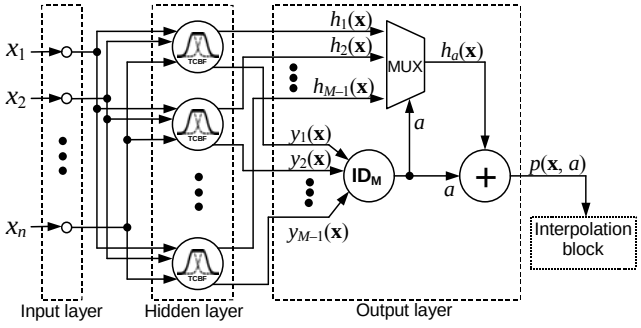

Fig. 6. The architecture of the expanded TCBF classifier with parameter identification functionality.

The classifier takes advantage of normalizing functions of TCBFs. Even though $h(\mathbf{x})$ is only an intermediate function in TCBF calculation algorithm, it has a property which can be useful in parameter identification. It follows from the fact that $h(\mathbf{x})$ describes position of a point $\mathbf{x}$ with reference to centers of a TCBF. The value is in the range from 0 to 1. If we assign one of object's parameter values to both centers of a TCBF than an actual parameter value for point $\mathbf{x}$ can be easily established e.g. through linear interpolation.

A construction procedure of the new classifier will be discussed on the basis of temperature identification problem in a compact smart resistance sensor with the anti-aliasing filter.

At the before-test stage, performed by simulation, the nominal identification curve for R_1 is evaluated according to the rules described in [12,13]. This curve illustrates state of the nominal anti-aliasing filter followed from changes of R_1 (the red curve shown in Fig. 7). Relation between points on the curve and temperature is defined by PN-EN 60751+A2. It can be used in an analytical way or through a conversion table consisting of a set of points: $\{(V_1, V_2) \rightarrow T\}$. The nominal curve is then divided into several sections in order to obtain a set of M points required to construct a classifier with $M - 1$ TCBFs. Obtained centers in the measurement space represented by digital codes of a 10-bit analog-to-digital converter are shown as red points in Fig. 7.

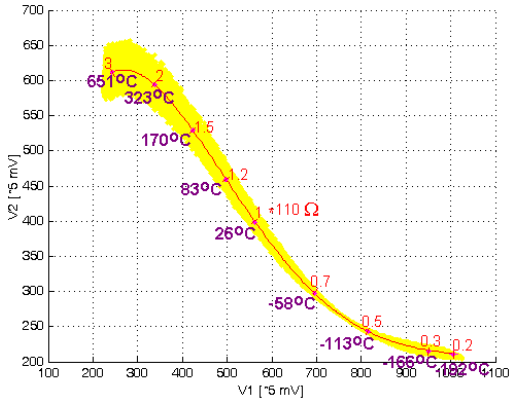

Fig. 7. Nominal and dispersed identification curve of parameter R_1 (Pt100) in the measurement space.

In the next step parameter tolerances in the anti-aliasing filter are introduced and a dispersed curve is generated (the yellow strip in Fig. 7). This curve is used to obtain scaling parameters σ and matrices $\mathbf{C}$ of TCBFs by means of statistical analysis [8].

At the after-test stage, for a measurement point $\mathbf{x}$ output values $y_m(\mathbf{x})$ of TCBFs are evaluated ($m = 1, 2, ..., M - 1$) and applied to inputs of a block marked as $\mathbf{ID_M}$ in Fig. 6. Its task depends on obtaining an index a of a TCBF with the greatest output value ($a = 1, 2, ..., M - 1$). This index firstly controls multiplexer (MUX) used for selection of the normalizing function value $h_a(\mathbf{x})$ of the winning TCBF. Secondly, it is combined with $h_a(\mathbf{x})$ in a summing block. As a result we obtain a new identification function $p(\mathbf{x}, a) = a + h_a(\mathbf{x})$. Since a value of $h_a(\mathbf{x})$ is in the range [0, 1], the new function is continuous in the range [1, M]. Finally, by means of an interpolation method, an actual temperature value $T = f(\, p(\mathbf{x}, a))$ can be obtained.

6. SIMULATION RESULTS

A set of 9 centers on nominal identification curve of the parameter R_1 was obtained for the anti-aliasing filter shown in Fig. 1. Hence, there are eight TCBFs in the architecture of the expanded TCBF classifier and value of the identification function $p(\mathbf{x}, a)$ ranges from 1 to 9 indicating position of the measurement point $\mathbf{x}$ with respect to the identification curve. Theoretical relation between temperature and value of the function $p(\mathbf{x}, a)$ is presented in Fig. 8.

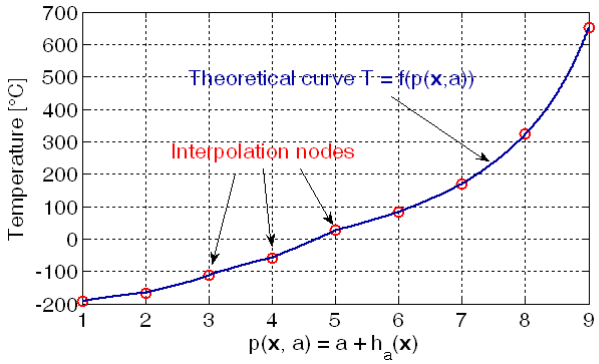

Fig. 8. Temperature value versus function $p(\mathbf{x}, a)$.

Different interpolation methods of the curve $T = f(p(\mathbf{x}, a))$ were compared in order to find out the lowest temperature identification errors. Nominal and dispersed identification curves were examined. Parameter tolerances 0.1 % for resistors and 0.2 % for capacitors were assumed. Results shown in Fig. 9 indicates that the highest temperature identification errors occurs with use of linear interpolation method for the last TCBF. It follows from the fact that the curve $T = f(p(\mathbf{x}, a))$ in this area is clearly nonlinear. The most even error level was obtained with use of a spline method. However for some TCBFs (e.g. 1st, 3rd) obtained errors are greater than with use of other methods.

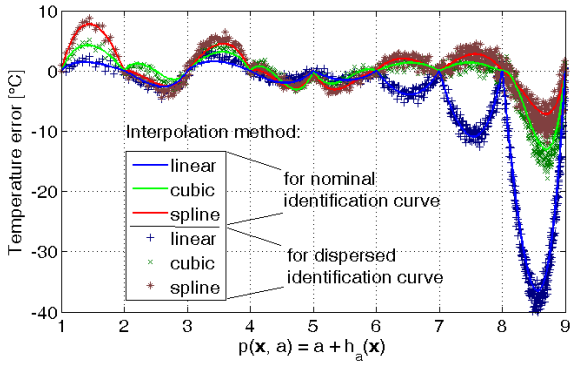

Fig. 9. Temperature error versus function $p(\mathbf{x}, a)$ of the classifier with 8 TCBFs for 850 simulations of different values of R_1 (tol_R = 0.1 %, tol_C = 0.2 %).

Preliminary simulations with three basic interpolation methods gave moderate results. In order to increase accuracy in the next step an approximation method with use of higher order polynomials obtained independently for each TCBF were applied. For parameters tolerances not greater than 0.2 % standard deviation of estimated temperature for the testing set containing 850 signatures equals 1 °C.

7. CONCLUSIONS

Presented solution with the resistance sensor embedded into the structure of an anti-aliasing filter of an ADC is an alternative for typical complex temperature measurement methods and is dedicated to low-power and low-cost applications. Temperature estimation accuracy achieved with use of the expanded TCBF classifier with parameter identification functionality, implemented algorithmically in the microcontroller, should be sufficient in applications where sensor must operate in a wide range of temperatures, but accuracy of parameter identification is a less critical parameter.

5. REFERENCES

[1] C. Eckert, R. Bax, “Practical RTD Interface”, National Semiconductor Corporation, Application Note 1559, June 2007.

[2] M. Leinonen, J. Juuti, H. Jantunen, “Interface circuit for resistive sensors utilizing digital potentiometers”, Sensors and Actuators A, vol. 138, issue 1, pp. 97–104, July 2007.

[3] F. Reverter, M. Gasulla, R. Pallàs-Areny, “Analysis of Power-Supply Interference Effects on Direct Sensor-to-Microcontroller Interfaces”, IEEE Transactions on Instrumentation and Measurement, vol. 56 no. 1, pp. 171-177, February 2007.

[4] F. Reverter, J. Jordana, M. Gasulla, R. Pallàs-Areny, “Accuracy and resolution of direct resistive sensor-to-microcontroller interfaces”, Sensors and Actuators A, vol. 121, issue 1, pp. 78–87, May 2005.

[5] F. Reverter and Ò. Casas, “Interfacing Differential Resistive Sensors to Microcontrollers: A Direct Approach”, IEEE Transactions on Instrumentation and Measurement, vol. 58 no. 10, pp. 3405-3410, October 2009.

[6] E. Sifuentesa, O. Casasa, F. Reverter, R. Pallàs-Areny, “Direct interface circuit to linearise resistive sensor bridges”, Sensors and Actuators A, vol. 147, issue 1, pp. 210-215, September 2008.

[7] J. Jordana, R. Pallàs-Areny, “A simple, efficient interface circuit for piezoresistive pressure sensors”, Sensors and Actuators A, vol. 127, issue 1, pp. 69-73, February 2006.

[8] M. Kowalewski, R. Zielonko, “A New Two-center Ellipsoidal Basis Function Neural Network for Fault Diagnosis of Analog Electronic Circuits”, Proceedings of the 2nd International Conference on Information Technology, Gdańsk, pp. 143-146, 2010.

[9] Z. Czaja, “A compact smart resistive sensor based on a microcontroller”, in Proc. of 14th Joint IMEKO TC1+TC7+TC13 Symposium, Jena, Germany, pp. 281-284, September 2011.

[10] Toczek W., Kowalewski M., “A neural network based system for soft fault diagnosis in electronic circuits”, Metrology and Measurement Systems, Vol. XII, iss. 4 (2005), pp. 463-476.

[11] Czaja Z., Kowalewski M., “An Application of TCRBF Neural Network in Multi-node Fault Diagnosis Method”, IMEKO XIX World Congress, pp. 503-508, Lisbon, Portugal, 2009.

[12] Z. Czaja, “A diagnosis method of analog parts of mixed-signal systems controlled by microcontrollers”, Measurement, vol. 40, issue 2, pp. 158-170, February 2007.

[13] Z. Czaja, “A method of fault diagnosis of analog parts of electronic embedded systems with tolerances”, Measurement, vol. 42, issue 6, pp. 903-915, July 2009.